



**"Gheorghe Asachi" Technical University of Iasi, Romania**



---

## TESTING ALGORITHMS FOR THE IDENTIFICATION OF ASBESTOS ROOFING BASED ON HYPERSPECTRAL DATA

Szilárd Szabó<sup>1\*</sup>, Péter Burai<sup>2</sup>, Zoltán Kovács<sup>1</sup>, György Szabó<sup>1</sup>,  
Attila Kerényi<sup>1</sup>, István Fazekas<sup>1</sup>, Mónika Paládi<sup>1</sup>, Tamás Buday<sup>1</sup>, Gergely Szabó<sup>1</sup>

<sup>1</sup>University of Debrecen, Institute of Geosciences, Egyetem sq. 1, 4032 Debrecen, Hungary

<sup>2</sup>Karoly Robert College, Research Institute of Remote Sensing and Rural Development, Hungary

---

### Abstract

There are several environmental issues in urban areas that are caused by the unintentional consequences of past activities. One of these issues is the wide application of asbestos cement in roofing materials in the 2<sup>nd</sup> half of the 1900s. In this study, our goal was to identify different roof types and to determine those with asbestos components using high-ground (1 m) and spectral (126 bands) resolution airborne hyperspectral imagery (AISA Eagle II) and several classification approaches. In addition, we aimed to identify those wavelengths that play a significant role in distinguishing the different roof types. In the image analysis, the SAM, MLC and SVM classification methods were used to evaluate the different types of roofs. These methods resulted in accurate maps of the roof types, and asbestos cement roofs were identified with over 85% accuracy.

**Key words:** Aisa EAGLE, asbestos-cement, hyperspectral remote sensing, image classification, roofs

Received: February, 2014; Revised final: October, 2014; Accepted: October, 2014

---

### 1. Introduction

During the second half of the 20<sup>th</sup> century, asbestos was a popular material as an additive in building materials (roofs, insulation) due to its good characteristics regarding resistance to heat (Bassani et al., 2007; Pascucci et al., 2010). Later, asbestos was determined to be composed of microscopic mineral fibers that are dangerous to people's health, causing asbestosis, lung cancer, and mesothelioma when inhaled into the lungs (Mádi et al., 2000; Petja et al., 2010). Accordingly, several European countries, including Hungary, have banned the usage of asbestos in all parts of life. Although a decree (EÜM-KöM, 2000) prohibited the distribution of asbestos roofing materials starting in 2001, there was a long grace period on the selling of stored stock: the final ban occurred in 2005.

Despite of the legal background, most people are unaware of the problem; thus, they may not properly handle the waste when they renovate their roofs. Accordingly, a thorough and exact register is required to determine the roofs that pose a risk of asbestos pollution (Field, 2009; Sokal and Rohlf, 2009).

Remote sensing provides effective tools to identify different urban surfaces, including roofing; furthermore, it can be used to identify asbestos materials. Most of the researchers who have applied remote sensing technology in an urban environment have focused on land cover, especially on green areas and their relevance in the ecological network (Chen et al., 2013; Rogan and Chen, 2003; Yang et al., 2003; Yang, 2011) or on monitoring the changes in the growth of towns by observing the built-in areas (Chen et al., 2000; Yang, 2011).

---

\* Author to whom all correspondence should be addressed: E-mail: szabo.szilard@science.unideb.hu; Phone: +36 52-512900/22326; Fax: +36 52 945

Urban surface analysis is a recent application of remote sensing data that is aimed to extract data on the artificial objects of cities. Differentiating roofing types using remotely sensed data can be an efficient means of establishing a register in a settlement. In addition to the asbestos issue, this register of roofs can have further practical applications, e.g., in fire risk assessment, it may provide direct information about the flammability of components and the possibilities of the spread of fire.

The spectral reflectance of materials is widely used in analytical procedures because this technique does not require expensive preparation (e.g., digestion), a process that may alter the analyzed materials itself. These non-destructive investigations can be conducted in the laboratory or in the field (Csillag et al., 1993; Bassani et al., 2007; Foudjo et al., 2013; Hărmănescu et al., 2012; Szalai et al., 2013) and are important in exploring the spectral features of “clear” substances and providing experience about the useful spectral ranges for aerial surveys.

There have been several successful attempts to identify roofs with remote sensing technology. Nagyvárdi et al. (2011) applied aerial images in the visible spectral range to identify buildings and their age (presuming that the roofs of older buildings had a darker red color); however, this type of data was not appropriate for the classification of different roof types. Taherzadeh et al. (2012) found Worldview-2 images to be useful in roof type detection; however, hyperspectral data provided better results. Cavalli et al. (2008) tested ALI, Hyperion, LANDSAT ETM+ and MIVIS data in an urban area and found that a resolution of 30 m was only able to identify the main land cover materials, whereas hyperspectral data (even with a coarse cell size) enabled more classes to be discriminated.

The best results were obtained using hyperspectral data. Shafri et al. (2012) summarized the possible applications of the hyperspectral data sources, and roof type classification was mentioned as

a reasonable application. Hyperspectral images are becoming increasingly available in the last few years and are slowly being used in several applications. However, there are limitations to obtaining clear results of roofing classification due to some independent factors.

(1) Different-aged roofs exhibit different colors (including all types of roofs) as they are exposed to weathering processes and UV radiation. (2) All roofs become covered by lichens and mosses (Bassani et al., 2007). (3) Almost all roofs have parts of different materials, such as valley gutters (metal), and sometimes there are windows (glass with plastic or wooden frame) with plastic or metal rolling shutters, making the pixels diverse and decreasing the homogeneity of the surface. (4) Roofs (except flat ones) have different geometrical shapes, which divides them into differently lightened regions. These regions can be very small, i.e., smaller than the resolution of the applied images. Due to these issues, roof classifications always have errors.

Our hypothesis was that roofs can be distinguished based on their spectral features; therefore, we aimed to produce a roof register with special regard to the identification of the AC roofs in a test area using hyperspectral imagery. Different classification algorithms were compared to reveal which one exhibited the best performance with special regards to the identification of asbestos materials in the roofs.

## 2. Methods

### 2.1. Data collection

We used airborne hyperspectral imagery of a 7-km<sup>2</sup> area of Debrecen, East-Hungary (Fig. 1). The city is the second largest in Hungary, with approximately 200,000 residents (Kozma, 2009) and has a diverse set of roofing types, ranging from the traditional red tiles to AC panels.

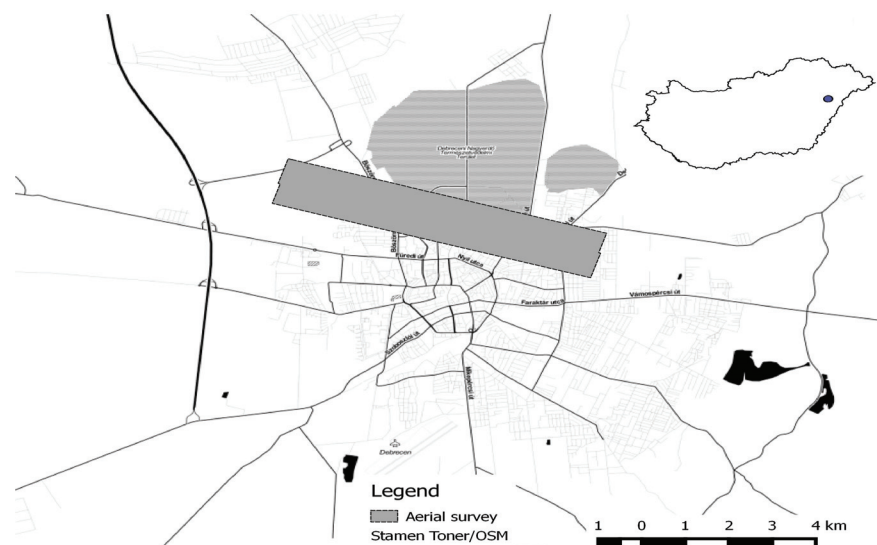


**Fig. 1.** Overview map of Debrecen city highlighting the area of the aerial survey

We used airborne hyperspectral imagery of an area of 7 km<sup>2</sup> of Debrecen (Fig. 1) that was captured using a push-broom type Aisa EAGLE II hyperspectral camera ([www.specim.fi](http://www.specim.fi)) during an aerial survey, which is capable of imaging in the visible to near-infrared spectral range (VNIR).

The acquisition of the images occurred between 08:12 and 08:46 GMT on 9th July, 2013. We applied 5-nm sampling in the full spectrum (400–1000 nm) such that each pixel contains 126 spectral channels. A high-accuracy OxTS RT 3003 GPS/INS system was used for recording the navigation data. The hyperspectral camera was mounted on the Piper Aztec type airplane. The image frames were merged into a mosaic after preprocessing; afterwards, we could use one image for the entire test area.

## 2.2. Image processing

Image analysis was performed using the ENVI+IDL 4.8 software. Because roofing types can be identified visually, we performed field observations; based on the observations, we extended our ground truth database to objects captured from aerial photographs. The coordinates of the observations were recorded with a pair of RTK GPS devices (one was used as a permanent station). The goal of the data collection was to provide the accurate teaching and monitoring areas required for the image analysis (Table 1). Training data were used in the classifications (teaching areas for the algorithms), whereas the ground truth data were the control in the accuracy assessments. The user's accuracy (UA), producer's accuracy (PA), overall accuracy (OA) and Kappa index were calculated (Congalton, 1991).

**Table 1.** Sizes of the training and ground data (number of pixels)

<b>Roof types</b>	<b>Ground truth</b>	<b>Training area</b>
Brown tile	56	114
Green tile	49	112
Asbestos	54	355
Light brown tar	12	29
Top, block of flats without insulation	90	443
Top, block of flats with insulation	115	139
Red tile	164	337

We collected data of all of the representative roofing types within the test area (Table 1). The most popular roofs were red tiles; however, especially in the case of newer houses, brown tiles were also widespread. Tar roofs denote a cheaper solution, but their life expectancy is shorter than that of tiles. Currently, according to the legal rules, the proportion of AC panels is not high, but several houses with these panels were observed. Using high-resolution aerial images (15-cm resolution), we discriminated between the surface of red tile roofs in sunlight and in shadows.

Several advanced feature extraction techniques have been developed to reduce the dimensionality of data. MNF transformation (Green et al., 1988) was applied to achieve noise reduction, and the new artificial bands, having the largest explained variance, were used in the classifications.

One of the most popular and useful hyperspectral image classification methods is the support vector machine (SVM) algorithm, which requires less prior knowledge to classify the high-dimensional nature of hyperspectral data (Camps-Valls and Bruzzone, 2005; Plaza et al., 2009). During image classification, we subjected the data to MNF transformation and applied pair-wise SVM and Maximum Likelihood (MLC) methods to 9 and 15 MNF bands. SVM classification was performed using the Gaussian Radial Basis Function (RBF) kernel with the following parameters: C=100 and  $\gamma=0.003$ . Furthermore, the spectral angle mapper (SAM) classifier was used in the analysis.

All classifications were conducted with a mask layer derived from a normalized Digital Surface Models (nDSM) and NDVI image of the same area. The nDSM was created by the simple subtraction of the DEM and DSM models (DSM-DEM). The NDVI was calculated using narrow bands in the red (677 nm) and near-infrared (801 nm) wavebands. An object-oriented image segment was delineated using a multi-resolution segmentation algorithm with eCognition 8. The segmented layer was classified such that segments with low NDVI values ( $NDVI<0.1$ ) paired with high nDSM ( $nDSM>3$  m) denoted a building with high probability.

## 3. Results

The spectral curves had unique features within the roofing types (Fig. 2); all of the curves within the types had distinct sections that can be used in multivariate classification algorithms. The best wavelength range to discriminate asbestos from the other materials was within the range of 580–800 nm; misclassification errors were caused by red tiles in shadows and by grey tar roof.

### 3.1. Roof classification and identification of asbestos

We experienced the weakest classification performance with the SAM method (OA: 59.83%, kappa: 0.54; Table 2). A relevant proportion of the control area remained unclassified due to the higher variance of the roofs of the test area (different age, roof aspect and slope) compared to the training area.

SVM provided better results, even when we used the original band set (OA: 79.93%, kappa: 0.77). MLC cannot be applied to the original dataset due to its limitations: we require a larger training pixel number than the number of investigated bands (i.e., the original band set). To reduce the dimensions, we applied the MNF transformation; thus, the first transformed bands contain most of the variance of the entire information ensured by the hyperspectral

survey. The use of the first 9 MNF bands with the MLC classifier was quite accurate (OA: 76.35%, kappa: 0.72), whereas the SVM results were similar to the results obtained for the original dataset (OA: 79.45%, kappa: 0.76%; Table 3; Fig. 3). The MLC and multiclass SVM methods resulted in almost the same accuracy using the MNF bands. The SVM method produced the best classification accuracy (OA: 79.9%) using the original (126) wavebands. Asbestos was identifiable with all of the methods (except the SAM): both the PA and UA were above 85%.

#### 4. Discussion

The differentiation of roofing types using remotely sensed data is a straightforward method of establishing cadasters in a settlement. Our hypothesis was proven regarding the ability of the roofing types to be separated based on remotely sensed data; also in addition, asbestos cement tiles can be identified with an acceptable accuracy (~85%, according to Anderson et al., 1976).

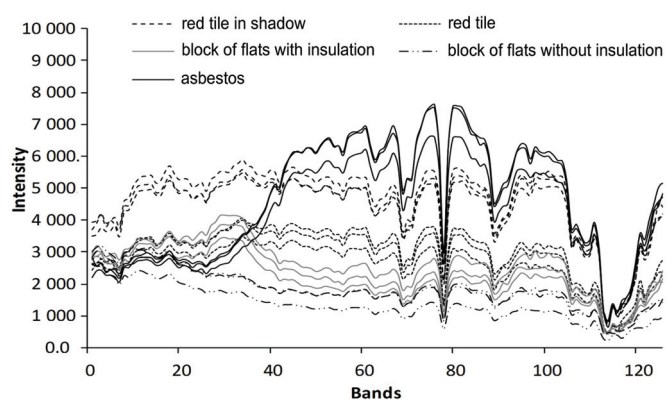


**Fig. 2.** Spectral curves of some representative roofing types in the study area (bands: 0=400 nm; 120=961 nm)

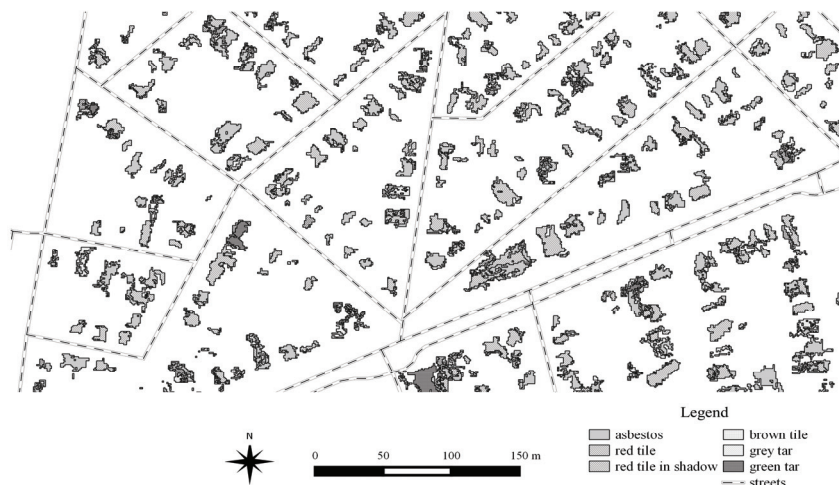


**Fig. 3.** Roofing types in the test area based on the SVM classification (using MNF-transformed data)

**Table 2.** Results of the accuracy of the classifications using the original 126 bands

Class	SAM (%)		SVM (%)	
	PA	UA	PA	UA
Brown tile	5.4	11.1	82.5	68.6
Green tile	60.0	100.0	86.6	100.0
Asbestos	23.0	90.2	50.4	93.1
Light brown tar	100.0	37.3	96.6	68.3
Top, block of flats without insulation	91.4	46.4	90.7	52.9
Top, block of flats with insulation	96.6	80.5	94.6	89.4
Red tile	1.0	65.2	85.2	91.1
Blue metal	63.2	95.0	88.0	91.2
Red tile in shadow	23.2	83.9	64.8	46.8
Grey tar	34.9	29.3	82.5	68.6
Overall accuracy (OA)	59.8		79.9	
Kappa index	0.54		0.77	

**Table 3.** Results of the accuracy of the classifications using MNF-transformed data

Class	SVM with 15 MNF bands (%)		MLC with 9 MNF bands (%)	
	PA	UA	PA	UA
Brown tile	97.6	71.3	54.5	88.4
Green tile	100.0	100.0	100.0	100.0
Asbestos	86.9	98.4	92.9	82.4
Light brown tar	96.6	100.0	3.6	100.0
Top, block of flats without insulation	89.2	99.2	92.1	88.3
Top, block of flats with insulation	98.6	85.3	77.7	79.6
Red tile	94.5	82.2	1.0	98.7
Blue metal	56.4	83.2	56.5	50.0
Red tile in shadow	47.7	55.4	26.8	60.0
Grey tar	28.7	22.1	36.1	38.5
Overall accuracy (OA)		79.5		76.3
Kappa index		0.76		0.72

The finer the spatial and spectral resolution of the data, the better the algorithms perform (Herold et al., 2002; Herold and Roberts, 2010; Taherzadeh et al., 2012; Tobak et al., 2012). According to Welch (1982), the minimum resolution for urban studies is at least 5 m; accordingly, our dataset had a resolution of 1 meter. However, we dealt with several issues that resulted in classification errors: despite the fine spatial resolution, roofs had complex geometrical shapes; as a result, the reflectance was spectrally mixed.

We applied hyperspectral data analysis using the original dataset and then analyzed the MNF-transformed data with the SAM, MLC and SVM algorithms. The SVM algorithm, with both the original dataset and the MNF-transformed data, exhibited the best performance. Brand (2012) also applied the SAM and SVM algorithms, and in her study, the SAM classifier performed better (OA was 70.5% for SAM and 59.06% for SVM).

Our results showed that the SVM algorithm exhibited better classification accuracy (OA: 79.9%), whereas the performance of SAM was the poorest (OA: 59.8%). Li et al. (2010) reached a similar conclusion, i.e., the SVM algorithm appeared to be the best algorithm for classifying impervious surfaces; presumably, SAM would provide better results with more types of roofing and better defined training areas.

## 5. Conclusions

In general, almost all roof types were identifiable with high accuracy from a hyperspectral image. The hyperspectral data provided sufficient accuracy for the mapping of asbestos materials using the SVM method with both the original band set and the MNF-transformed data; MLC was applied only with the MNF-transformed data, and its accuracy was almost the same as that of SVM.

Although SAM is regarded as a good classifier, it exhibited poor performance in this study.

## Acknowledgements

This paper was supported by TÁMOP-4.2.2.A-11/1/KONV-2012-0041. The project was subsidized by the

European Union and co-financed by the European Social Fund.

## References

- Anderson J.R., Hardy E.E., Roach J.T., Witmer R.E., (1976), *A Land Use and Land Cover Classification System for Use With Remote Sensor Data*, Geological Survey Professional Paper 964, United States Government Printing Office, Washington, 41.
- Bassani C., Cavalli R.M., Cavalcante F., Cuomo V., Palombo A., Pascucci S., Pignatti S., (2007), Deterioration status of asbestos-cement roofing sheets assessed by analyzing hyperspectral data, *Remote Sensing of Environment*, **109**, 361-378.
- Camps-Valls G., Bruzzone L., (2005), Kernel-based methods for hyperspectral image classification, *IEEE Transactions on Geoscience and Remote Sensing*, **43**, 1351-1362.
- Cavalli R.M., Fusilli L., Pascucci S., Pignatti S., Santini F., (2008), Hyperspectral sensor data capability for retrieving complex urban land cover in comparison with multispectral data: Venice City case study (Italy), *Sensors*, **8**, 3299-3320.
- Chen S., Zeng S., Xie C., (2000), Remote sensing and GIS for urban growth analysis in China, *Photogrammetric Engineering and Remote Sensing*, **66**, 593-598.
- Chen Z., Yuan L., Shihai L., Jiande F., Yanguo T., Haibo Z., Daiqing L., (2013), Evaluation of urbanized ecological environment quality: a case study on Beijing Chaoyang District, *Environmental Engineering and Management Journal*, **12**, 1779-1784.
- Congalton R.G., (1991), A review of assessing the accuracy of classifications of remotely sensed data, *Remote Sensing of Environment*, **37**, 35-46.
- Csillag F., Pásztor L., Biehl L., (1993), Spectral band selection for the characterization of salinity status of the soil, *Remote Sensing of the Environment*, **43**, 231-242.
- EüM-KöM, (2000), EuM-KöM decree on the limitations of the activities with dangerous materials and products (in Hungarian), 41/2000, *Magyar Közlöny*, **125**.
- Field A., (2009), *Discovering Statistics*, SAGE Publications, London.
- Foudjo B.U.S., Kansci G., Lazar I.M., Lazar G., Fokou E., Etoa F-X., (2013), ATR-FTIR characterization and classification of avocado oils from five cameroon cultivars extracted with a friendly environmental

- process, *Environmental Engineering and Management Journal*, **12**, 97-103.
- Green A.A., Berman M., Switzer P., Craig M.D., (1988), A transformation for ordering multispectral data in terms of image quality with implications for noise removal, *IEEE Transactions on Geoscience and Remote Sensing*, **26**, 65-74.
- Hărmănescu M., Alexandru M., Gergen I., (2012), FTIR spectroscopy – a nondestructive method to monitor the impact of different fertilizers on the floristic matrix of permanent grassland, *Environmental Engineering and Management Journal*, **11**, 351-357.
- Herold M., Gardner M., Hadley B., Roberts D., (2002), *The Spectral Dimension in Urban Land Cover Mapping from High-Resolution Optical Remote Sensing Data*, Proc. of the 3rd Symposium on Remote Sensing of Urban Areas, June 2002, Istanbul, Turkey, 8.
- Herold M., Robert, D., (2010), *The Spectral Dimensions in Urban Remote Sensing*, In: *Remote Sensing of Urban and Suburban Areas*, Springer, Dordrecht-Heidelberg-London-New York, 47-65.
- Kozma G., (2009), Place marketing in Hungary: a case study of Debrecen, *European Spatial Research and Policy*, **16**, 59-74.
- Li P., Xu H., Li S., (2010), *Urban Impervious Surface Extraction from very High Resolution Imagery by One-Class Support Vector Machine*, ISPRS TC Symposium, Vienna, Austria, IAPRS, 38 Part B, 366-370.
- Mándi A., Posgay M., Vadász P., Major K., Rödelsperger K., Tossavainen A., Ungváry G., Woitowitz H.J., Galambos E., Németh L., Soltész I., Egerváry M., Böszörmenyi Nagy G., (2000), Role of occupational asbestos exposure in Hungarian lung cancer patients, *International Archives of Occupational and Environmental Health*, **73**, 555-560.
- Nagyváradi L., Gyenizse P., Szabényi A., (2011), Monitoring the changes of a suburban settlement by remote sensing, *Acta Geographica Debrecina Landscape and Environment*, **5**, 76-83.
- Pascucci S., Bassani C., Cavalli R.M., Fusilli L., Palombo A., Pignatti S., Santini F., (2010), *Hyperspectral Remote Sensing Capability for Mapping Near-Surface Asbestos-Deposits and Pollutants Dispersion in Soils*, Proc. Hyperspectral 2010 Workshop, Frascati, Italy.
- Petja P.M., Twumasi Y.A., Tengbeh G.T., Atanasova M., (2010), Spatial epidemiology risk assessment for rehabilitated former asbestos mining areas in Limpopo Province, South Africa, using remote sensing and conventional analytical methods, *South African Journal of Epidemiology and Infection*, **25**, 32-39.
- Plaza A., Benediktsson J.A., Boardman J.W., Brazile J., Bruzzone L., Camps-Valls G., Chanussot J., Fauvel M., Gamba P., Gualtieri J., Marconcini M., Tilton J.C., Trianni G., (2009), Recent advances in techniques for hyperspectral image processing, *Remote Sensing of Environment*, **113**, 110-122.
- Rogan J., Chen D.M., (2003), Remote sensing technology for mapping and monitoring land cover and land use change, *Progress in Planning*, **61**, 301-325.
- Shafri H.Z.M., Taherzadeh E., Mansor S., Ashurov R., (2012), Hyperspectral remote sensing of urban areas: an overview of techniques and applications, *Research Journal of Applied Sciences, Engineering and Technology*, **4**, 1557-1565.
- Sokal R.R., Rohlf F.J., (2009), *Introduction to Biostatistics*, Dover Publications, Inc., New York, USA.
- Szalai Z., Kiss K., Jakab G., Sipos P., Belucz B., Németh T., (2013), The use of UV-VIS-NIR reflectance spectroscopy to identify iron minerals, *Astronomical Notes*, **334**, 940-943.
- Taherzadeh E., Shafri H.Z.M., Soltani S.H.K., Mansor S., Ashurov R., (2012), *A comparison of hyperspectral data and Worldview-2 images to detect impervious surface*, ASPRS Annual Conference, March 19-23, Sacramento, California, On line at: [http://www.asprs.org/a/publications/proceedings/Sacramento2012/files/Taherzadeh\\_2%28oral%29.pdf](http://www.asprs.org/a/publications/proceedings/Sacramento2012/files/Taherzadeh_2%28oral%29.pdf).
- Tobak Z., Cséndes B., Henits L., van Leeuwen Boudewijn, Szatmári J., Mucsi L., (2012), *Examination of urban surfaces' spectral characteristics using aerial imaging*, Proc. VI. Hungarian Conference on Geography, Szeged, Hungary, 1088-1097.
- Welch R., (1982), Spatial resolution requirements for urban studies. *International Journal of Remote Sensing*, **3**, 139-146.
- Yang L., Xian G., Klaver J.M., Deal B., (2003), Urban land cover change detection through sub-pixel imperviousness mapping using remotely sensed data, *Photogrammetric Engineering and Remote Sensing*, **69**, 1003-1010.
- Yang X., (2011), *Urban Remote Sensing: Monitoring, Synthesis and Modelling in the Urban Environment*, Wiley, New York.